

## Geoneutrino: models and data

---

**Smirnov Oleg**<sup>\*†</sup>

*JINR Dubna, Russia*

*E-mail: osmirnov@jinr.ru*

Geo-neutrinos, the antineutrinos from beta- decaying elements in  $^{238}\text{U}$ ,  $^{232}\text{Th}$  chains and  $^{40}\text{K}$  decays in the Earth, are the only reliable sources of information on the distribution and concentration of these elements in the entire planet. Their detection can shed the light on the sources of the terrestrial heat flow, on the present composition, and on the origins of the Earth.

Although geo-neutrinos were conceived long ago, a first detection of the geoneutrinos occurred very recently due to the development of large volume ultrapure liquid scintillator detectors. This year the Borexino and KamLAND had reported 99.997% C.L. for the presence of non-zero geoneutrino signal in their registered antineutrino spectra, opening a new era in geophysics.

Geoneutrinos, if registered with appropriate precision, potentially can help to answer the questions regarding our planet: what is the radiogenic contribution to terrestrial heat production; what is the content of U and Th in the crust and in the mantle respectively; is there any hidden source of heat in the Earth's core, such as a geo-reactor or  $^{40}\text{K}$ ; and, finally, is the standard geochemical model (the so called Bulk Silicate Earth model) consistent with geo-neutrino data?

*The Xth Nicola Cabibbo International Conference on Heavy Quarks and Leptons,  
October 11-15, 2010  
Frascati (Rome) Italy*

---

<sup>\*</sup>Speaker.

<sup>†</sup>

## 1. Introduction

Geo-neutrinos are (anti)neutrinos from  $\beta$ -decaying elements in the Earth. The main contribution comes from the decay chains of  $^{238}\text{U}$  and  $^{232}\text{Th}$ , and  $^{40}\text{K}$  decays, with negligible contribution from  $^{87}\text{Rb}$  and  $^{235}\text{U}$  chain. The Earth emits (mainly) antineutrino, the expected flux at the surface of the Earth is  $\sim 10^6 \text{ cm}^{-2}\text{s}^{-1}$ . Decays of the natural radioactive elements contribute to the terrestrial heat production.

Geo-neutrino flux measurements do provide experimental evidence for the quantity and distribution of radioactive elements internally heating the Earth, while the direct measurement of the composition is possible for the crust only. Radiogenic heating helps power plate tectonics, hot-spot volcanism, mantle convection, and possibly the geo-dynamo. Information on the extent and location of this heating better defines the thermal dynamics and chemical composition of Earth.

Geoneutrinos, if registered with appropriate precision, potentially can help to answer the open questions regarding the natural radioactivity in our planet: what is the radiogenic contribution to terrestrial heat production; how much U and Th the crust contains; how much U and Th the mantle contains; is there any georeactor or  $^{40}\text{K}$  excess hidden in the Earth's core as believed by some authors; is standard geochemical model (the so called Bulk Silicate Earth model) consistent with geo-neutrino data?

## 2. Models

A model providing abundances of radioactive elements in every region of the Earth is necessary for the calculation of the expected geoneutrino signal. The Earth structure as follows from seismic data consist of 5 basic regions: inner core, outer core, mantle, oceanic crust, and continental crust and sediments. The seismic data doesn't provide however the composition of these regions. A global description of the present crust-plus-mantle system is generally provided by the Bulk Silicate Earth model (BSE), a reconstruction of the primordial mantle of the Earth, subsequent to the core separation and prior to crust differentiation. The model is based on chondrite meteorites composition (undifferentiated meteorites that do not show any evidence of having been melted since the formation of their parent bodies) and geochemical arguments. The homogeneous composition of seismically bounded regions is typically assumed for modeling. The abundance of the U/Th in the inner regions is derived from the composition of meteorites in assumption that the Earth has the same composition as the Solar system. The BSE model provides the total amount of U,Th and K in the Earth, as these lithophile elements should be absent in the core. The BSE is consistent with most observation concerning crust and upper mantle.

Models presented so far by different authors [1, 2, 3, 4] are based on the geophysical  $2^\circ \times 2^\circ$  crustal map [5] and on the density profile of the mantle as given by the 1d spherically symmetric model, the so called Preliminary Reference Earth Model (PREM) [6]. Geoneutrino signal predicted by these models are in good agreement. The difference within 10% is due to the adopted abundances of U and Th in the crust and upper mantle, and due to the model of mantle. All calculations use the BSE mass constraint in order to determine the abundances in the lower portion of the mantle. Applying mass balance relationships to estimate uranium and thorium content in various Earth reservoirs, one can predict the distribution of these elements and the resulting geo-neutrino

flux. The mass ratios within the BSE are:  $M(\text{Th})/M(\text{U}) = 3.9$ ,  $M(\text{K})/M(\text{U}) \approx 10^4$  and U abundance is  $2 \cdot 10^{-8}$ , concentration of U in the mantle is 0.01 ppm. In the BSE model the present radiogenic production of 19 TW is mainly from U and Th, and accounts for about one half of the total heat flow.

The minimal amount of radioactive elements in the Earth is the one compatible with lower bounds on measured abundances of natural radioactivity in the crust (minimal radiogenic model). On the other hand, the maximum amount of radioactive elements is provided by the global terrestrial heat flow of 44 TW, the radiogenic heat production can't exceed the measured value. This provides fully radiogenic model: a model with radiogenic heat production only, where K/U ratio is fixed at the terrestrial value and Th/U ratio is fixed at the chondritic value (consistent with terrestrial). Abundances are rescaled to provide the full 44 TW heat flow. The minimal radiogenic to fully radiogenic interval is rather large and can be reduced using geo-neutrino data.

Half of the total geoneutrino signal is expected from the local region, from the distance of the order of some hundredth kilometers. The study of regional geology is needed in order to improve the predictions of the reference model.

For comprehensive review of geo-neutrinos see [7].

### 3. Detectors

A fraction of  $^{238}\text{U}$  and  $^{232}\text{Th}$  antineutrino energy spectrum is above 1.8 MeV, which makes possible their detection with liquid organic scintillators via the reaction of inverse beta-decay on proton  $\bar{\nu}_e + p \rightarrow e^+ + n$  (1.8 MeV threshold). Positron annihilation gives prompt signal and the neutron capture after some hundredth microseconds provides a delayed signal. In position-sensitive ultrapure liquid scintillator detectors these process can be effectively recognized.

At present two collaborations, KamLAND and Borexino, have reported the geoneutrino measurement. Both experiments are exploiting large volume liquid scintillator detectors, with 1000 and 300 tones of target mass correspondingly, placed deep underground to protect the setup against the cosmic muons. The antineutrino detection is performed via inverse beta decay on proton, the details of the candidate selection are reported in Table.1. The Borexino energy selections are performed using the measured photoelectrons yield, while KamLAND uses the reconstructed energy. The efficiency of the candidates selections (1-4 in the table) is higher in Borexino (85%), KamLAND reports 70% efficiency. The selection of the FV decreases the amount target protons: in Borexino the outer layer of 25 cm is removed, and in KamLAND 50 cm layer is removed (in the first analysis the thicker layer of 150 cm was removed). The Borexino spatial selection doesn't assume sphericity of the detector and is performed using the measured shape of the inner vessel. Cut #6 serves to remove possible contamination of the sample with short-lived ( $\beta n$ )-decaying cosmogenic isotopes (2 seconds after the muon crossing the detector) and background induced by muons passing through the buffer (2 ms veto), mainly due to the neutrons production. For the crossing muons the KamLAND used more advanced selections to select showering muons only, this results in moderate loss of 4% live-time in comparison to 10% of the Borexino case, the difference per crossing muon is even bigger if we take into account the higher muons flux at the Kamioka site.

	Borexino	KamLAND-I	KamLAND-II
	$\sim 500$ p.e./MeV 438 p.e./2x511 MeV $\gamma$	$\sim 250$ p.e./MeV	$\sim 250$ p.e./MeV
1	$Q_p > 410$ p.e.	$0.9 < E_p < 2.6$ MeV	$0.9 < E_p < 2.6$ MeV
2	$700 < Q_d < 1250$ p.e.	$1.8 < E_d < 2.6$ MeV	$1.8 < E_d < 2.6$ MeV or $4.0 < E_d < 5.8$ MeV
3	$\Delta R < 1$ m	$\Delta R < 1$ m	$\Delta R < 2$ m
4	$20 < \Delta T < 1280$ $\mu$ s ( $T_{1/2} = 256$ $\mu$ s)	$0.5 < \Delta T < 500$ $\mu$ s ( $T_{1/2} = 207.5 \pm 2.8$ $\mu$ s)	$0.5 < \Delta T < 1000$ $\mu$ s ( $T_{1/2} \simeq 207.5 \pm 2.8$ $\mu$ s)
5	$R_{IV}(\Theta, \phi) - R_p(\Theta, \phi) > 0.25$ m	$R_p < 5$ m and $R_d < 5$ m	$R_p < 6$ m and $R_d < 6$ m
6	$T_\mu > 2$ s (for every muon passing through the detector, 10% live time loss) + $T_\mu > 2$ ms	$T_\mu > 2$ s (“showering muons”, 4% live time loss) + $T_\mu > 2$ ms	$T_\mu > 2$ s (“showering muons”, 4% live time loss) + $T_\mu > 2$ ms
	$\varepsilon(1-4) = 0.85 \pm 0.01$	$\varepsilon(1-4) = 0.697 \pm 0.007$	

**Table 1:** Antineutrino candidates selection in KamLAND and Borexino detectors. Indexes “p” and “d” stays for the prompt and delayed events. Borexino performs selections in the “light yield scale” (measured in photoelectrons, p.e.);  $\Delta R$  is the reconstructed distance between prompt and delayed events;  $\Delta T$  is time difference between the prompt and delayed events;  $R_{IV}(\Theta, \phi)$  in the Borexino case is the radial position of the inner vessel (IV) in the direction  $(\Theta, \phi)$ ;  $T_\mu$  is time passed after preceding muon;  $\varepsilon$  is selections efficiency. The selection criteria for KamLAND have changed since the first analysis, we are showing here both sets. In the last case efficiency is energy dependent and varies from 0.3 at the threshold to  $\sim 0.8-0.9$  for higher energies. The radius of the KamLAND inner vessel is  $R_{det} = 6.5$ m.

#### 4. Backgrounds

Principal backgrounds in the geoneutrino search are:

**Reactor antineutrinos.** For KamLAND measurements they contribute 81% of the total antineutrino signal in KamLAND geo-nu window [0.9-2.6 MeV] and only  $\sim 36\%$  for the Borexino case. Geo/Reactor antineutrino ratio is 0.23 in KamLAND versus 1.8 in Borexino site (because of the presence of other backgrounds it is different from the signal-to-noise ratio).

**Cosmic muons induced backgrounds,** including cosmogenic production of  $(\beta n)$ -decaying isotopes. At LNGS the muons flux is of about factor 7 lower than at the Kamioka site.

**Internal radioactive contamination:** accidental coincidences and  $(\alpha n)$ -reaction on  $^{13}\text{C}$ , monoenergetic  $\alpha$  with energy of 5.4 MeV are produced in  $^{210}\text{Po}$  decays. Borexino typical contamination is 3-4 orders of magnitude lower; KamLAND is now purifying the LS, factor 20 on  $(\alpha n)$  reduction is already achieved as reported in [8].

The main backgrounds for both experiments, excluding nuclear reactors signal, are listed in Table.2. The main source of background in KamLAND is  $(\alpha n)$ -reaction on  $^{13}\text{C}$ . Another significant source of background in KamLAND are accidental coincidences. The both backgrounds are much lower in Borexino.

#### 5. Measurements and comparison to model

In 2005 the first indication of the non-zero geoneutrino signal on the data set from  $7.09 \times 10^{31}$

Source	Borexino [events/(kt-yr)]	KamLAND [events/(kt-yr)]
Cosmogenic ${}^9\text{Li}$ and ${}^8\text{He}$	$0.3 \pm 0.2$	$0.48 \pm 0.025$
Fast neutrons from muons in water tank	<0.1 (measured)	<0.7
Fast neutrons from muons in rocks	<0.4 (MC)	
Non-identified muons	$0.11 \pm 0.01$	
Accidental coincidences	$0.80 \pm 0.01$	$18.76 \pm 0.025$
Time correlated background	<0.26	
( $\gamma$ n)-reactions	<0.003	
Spontaneous fission in PMTs	$0.030 \pm 0.003$	
( $\alpha$ ,n)-reaction in LS ( ${}^{210}\text{Po}$ )	$0.14 \pm 0.01$	$40.1 \pm 4.4$
( $\alpha$ ,n)-reaction in buffer ( ${}^{210}\text{Po}$ )	<0.61	
Total	$1.4 \pm 0.2$	$59.3 \pm 4.4$
Signal (measured)	$39^{+16}_{-13}$ (with 0.2526 kt-yr)	$25.7^{+7.0}_{-6.8}$ (with 4.126 kt-yr)

**Table 2:** Backgrounds in KamLAND and Borexino detectors

target proton years was reported by KamLAND [9], 90% confidence interval for the total number of detected geoneutrinos of 4.5 to 54.2 was found with the U/Th ratio fixed at 3.9. Updated result with  $2.44 \times 10^{32}$  proton-yr exposition for combined U+Th best-fit value flux of  $(4.4 \pm 1.6) \times 10^6 \text{ cm}^{-2} \text{ s}^{-1}$  ( $73 \pm 27$  events) was reported later [10], again with fixed U/Th ratio.

In April 2010 the first high significance confirmation on the geoneutrino signal come from Borexino [11], the collaboration reported  $9.9^{+4.3(15.8)}_{-3.4(8.0)}$  registered geoneutrino events at 68% C.L. (99.73%). The Borexino observed spectrum is presented in Fig.1 (left). In the absence of independent measurement of the reactor antineutrino the analysis was performed with unconstrained reactor antineutrino flux. The presence of non-zero geoneutrino signal was confirmed at the 99.997% level. Though measured with the lower exposition compared to the KamLAND, the result has higher statistical significance due to the much better signal-to-noise ratio. As can be seen in Fig.1 (right), the best-fit value of measured flux corresponds to fully radiogenic model, but the measurement is compatible with predictions of BSE model at  $1\sigma$  level.

The last news come again from KamLAND, preliminary analysis of  $3.49 \cdot 10^{32}$  proton-yr exposition was presented at Neutrino-2010 conference [8]. The rate-only analysis lead to  $111^{+45}_{-43}$  geo-neutrino events, with null-signal excluded at 99.95%. The operational troubles at the power reactors after serious earthquake in 2007 caused lower reactor neutrino flux in this period. KamLAND has experienced large known time variation of the background. This helped in extracting constant contribution from geo-neutrinos which can be seen above the estimated reactor neutrino + non-neutrino background in the geo-neutrino energy range, 0.9 - 2.6 MeV. Taking the advantage of timing information, the presence of non-zero geoneutrino signal was confirmed at the 99.997% level, the same as reported earlier by Borexino. The results are shown in Fig.2. The first attempt of the analysis of the KamLAND data with free U/Th ratio is shown in the right plot of Fig.2. As one can see in the plot, zero contribution of U or Th is still compatible with the data at  $1\sigma$  level.

The power of hypothetical georeactor at the center of the Earth can be constrained using the geoneutrino data. Borexino set an upper bound for a 3 TW geo-reactor at 95% C.L. by comparing

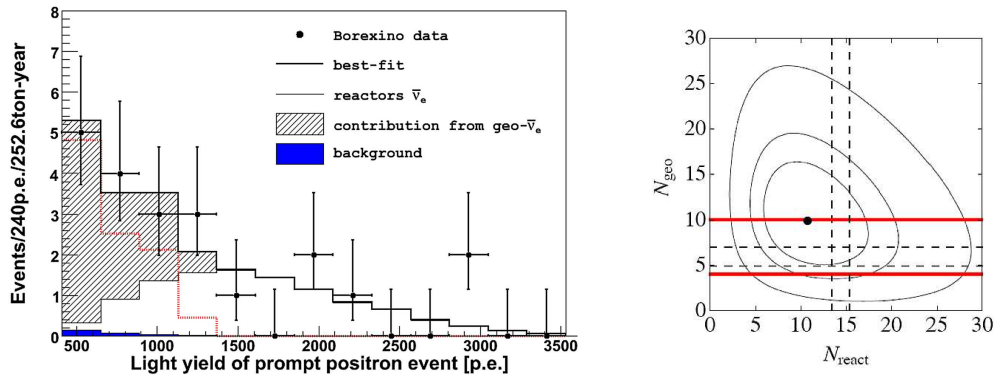


**Figure 1: Left:** light yield spectrum for the positron prompt events of 21 antineutrino candidates and the best-fit (solid thick line). The horizontal axis shows the number of p.e. detected by the PMTs. The small filled blue area on the lower left part of the spectrum is the background. Thin solid line: reactor antineutrino signal from the fit. Dotted line (red): geo-neutrino signal resulting from the fit. The darker area isolates the contribution of the geo-neutrino in the total signal. The conversion from p.e. to energy is approximately 500 p.e./MeV. **Right:** allowed regions for  $N_{geo}$  and  $N_{reactor}$  at 68%, 90% and 99,73% from the Borexino data fit. Horizontal and vertical dashed lines constrain the  $1\sigma$  regions for the geoneutrino (based on BSE model predictions) and expected number of reactor antineutrinos (taking into account oscillations). Horizontal solid red lines: predictions of the Fully and Minimal Radiogenic Earth models.

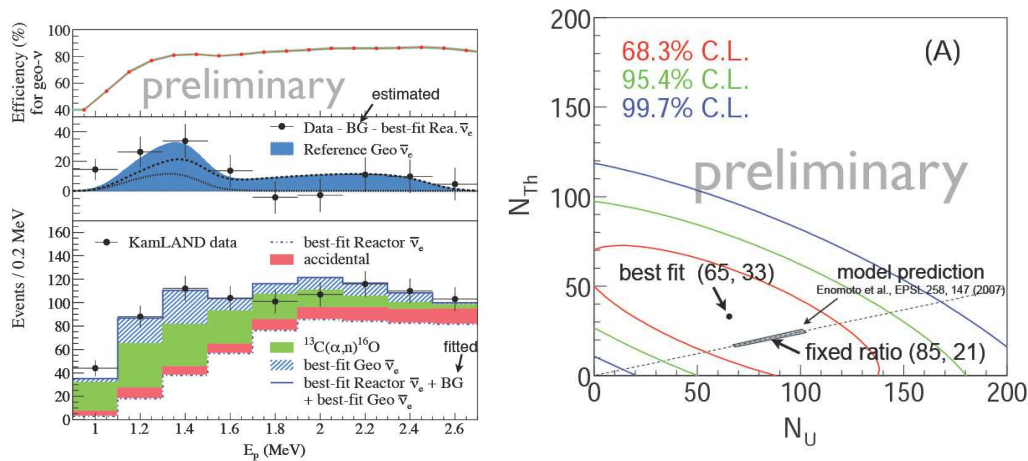


**Figure 2: Left:** KamLAND (preliminary) data in the geo-neutrino energy window (0.9-2.6 MeV). The extracted geoneutrino best-fit spectrum is shown in blue. **Right:** allowed regions for  $N_{Th}$  and  $N_U$  at 68%, 90% and 99,73% from the KamLAND data fit. The measurement is in agreement with the reference model.

the number of expected (from reactors + geo-reactor and background) and measured events in the reactor antineutrino energy window. Previously, this hypothesis had been studied with KamLAND data, and a limit of 6.2 TW was obtained at 90% C.L.

### 6. Future projects

SNO+ solar neutrino detector, nearing the completion at Sudbury laboratory, will be the next

detector capable to register geoneutrino [12]. It is located at deep Sudbury mine, at 6010 m.w.e (70 muons a day), and will operate 780 tonnes LAB- based liquid scintillator detector. 29 geoneutrino events per live-year are expected compared with 26 events from reactors in the same energy range. The measurement with SNO+ is very promising due to the very low flux of muons, another advantage is also the profound geological studies in the local region (the Sudbury itself is a mine). The scintillation filling is planned for spring 2012.

LENA is a project of 50 ktone deep underground multipurpose liquid scintillator detector waiting for funding [13]. About 1500 geoneutrino events per year are expected.

Hanohano is a project of underwater 10 ktone liquid scintillator detector [14]. The Hanohano should be a portable device deployed from the barge. It is aimed to extract mantle contribution in the total geoneutrino signal, which is very important from the geophysical point of view. About 100 geoneutrino events per year are expected.

The combination of data from multiple sites and data from an oceanic experiment would provide valuable information for geological models.

## 7. Conclusions

Geoneutrino existence is confirmed at  $4.2\sigma$  (99.997%) level independently by Borexino and KamLAND. The precision of both available measurements (Borexino and KL) is still too low: ~40% and 27% correspondingly for U+Th signal, and much worse for the unconstrained R(U) and R(Th) measurements. Different geological models for the moment can't be discriminated by existing measurements, more precise measurements are needed. Regional measurements in location of experiments are needed to provide more precision for the models. Independent measurements at various sites are highly desirable to check contributions from crust/mantle. We are expecting more input for the geological models from future detectors.

## References

- [1] F. Mantovani, L. Carmignani, G. Fiorentini, M. Lissia, Phys. Rev. D 69 (2004) 013001.
- [2] S. Enomoto, E. Ohtani, K. Inoue and A. Suzuki, Earth Planet. Sci Lett. 258 (2007) 147.
- [3] L. Fogli, E. Lisi, A. Palazzo and A. M. Rotunno, Earth Moon Planets 99 (2006) 111.
- [4] S.T. Dye, Earth and Planetary Science Letters 297 (2010) 1.
- [5] C. Bassin, G. Laske and G. Masters, EOS Trans. AGU 81 (2000) F897 ; G. Laske, G. Masters and C. Reif, "Crust 2.0 a new global crustal model at  $2 \times 2$  degrees", 2001, available online at <http://igppweb.ucsd.edu/~gabi/crust2.html>.
- [6] A. M. Dziewonski and D. L. Anderson, Phys. Earth Planet. Inter. 25 (1981) 297.
- [7] G. Fiorentini, M. Lissia and F. Mantovani, Phys. Rep. 453 (2007) 117.
- [8] K. Inoue, Neutrino-2010, "New Geo-neutrino Measurement with KamLAND", <http://www.neutrino2010.gr/>.
- [9] T. Araki *et al.*, KamLAND collaboration, Nature 436 (2005) 499.
- [10] S. Abe *et al.*, KamLAND collaboration, Phys.Rev.Lett. 100 (2008) 221803.
- [11] G. Bellini *et al.*, Borexino collaboration, Phys.Lett. **B687** (2010) 299.
- [12] M. Chen "SNO+: status and prospects", Neutrino Geoscience 2010; <http://geoscience.lngs.infn.it/>
- [13] F. von Feilitzsch "LENA: status and prospects", Neutrino Geoscience 2010; <http://geoscience.lngs.infn.it/>
- [14] J. Learned "Towards Hanohano", Neutrino Geoscience 2010; <http://geoscience.lngs.infn.it/>